ciency is high for $M = 15$ because the BG wave is not highly excited. The efficiency decreases drastically for $M = 5$ due to the high excitation of the BG wave coming from the overlap of both responses.

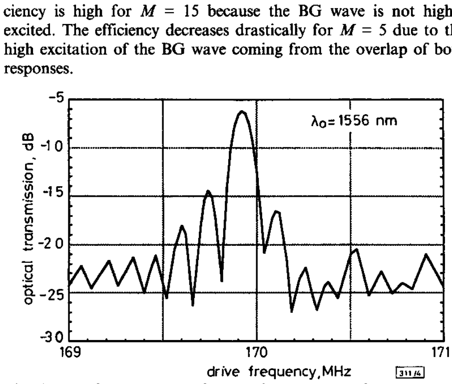

Fig. 4 *Optical transmission of AOTF between two polarisation maintaining fibres and cross-polarisers*

Electric drive power is 6mW

Design and realisation of AOTF: To have low drive power, the number of electrode pairs must be as large as possible but compatible with the desired AOTF tunability. In our case $M = 15$ is chosen because 100nm of tunability is sufficient for multiplexed communications [9]. Fig. 4 shows the measured optical response of the AOTF depicted in Fig. 1. The transducer fingers are inclined by 4.5° to compensate for the acoustic propagation walkoff [2] and the aperture is 100μm; its admittance response is plotted in Fig. 3. An acoustic waveguide [3] is fabricated by indiffusion of titanium (1800Å at 1030°C for 40h) and defines a 3cm interaction length. Impedance matching to the 50Ω of the generator is realised by a T network (two series inductors and one shunt capacitor). The optical waveguide (8.5μm wide) is made by standard Ti-indiffusion (1000Å at 1030°C for 10h). Under these conditions, the electric drive power is only 6mW for complete conversion.

Conclusion: We have pointed out that transducers on $LiNbO_3$ using the current X-cut Y-propagation for AOTF, create Bleustein-Gulyaev SAWs. This fact has generally little influence on the acousto-optic response but decreases the acoustic efficiency. To obtain low drive power, the number of electrode pairs must be as great as possible (small bandwidth) depending on the required AOTF tunability. An AOTF has been realised with an RF drive power of 6mW which is, to our knowledge, the lowest value reported to date.

Acknowledgments: The authors wish to thank J.C. Jacquinot for the electrical matching network and G. Soulage for some AOTF characterisations.

15 May 1995

Electronics Letters Online No: 19950851

C. Duchet, C. Brot and M. Di Maggio (*Alcatel Alsthom Recerche, Route de Nozay, 91460 Marcoussis, France*)

References

1 HEFFNER, B.L., SMITH, D.A., BARAN, J.E., YI-YAN, A., and CHEUNG, K.: 'Integrated-optic acoustically tunable infra-red optical filter', *Electron. Lett.*, 1988, **24**, pp. 1562–1563

2 FRANGEN, J., HERRMANN, H., RICKEN, R., SEIBERT, H., SOHLER, W., and STRAKE, E.: 'Integrated optical, acoustically tunable wavelength filter', *Electron. Lett.*, 1989, **23**, pp. 1583–1584

3 SMITH, D.A., and JOHNSON, J.J.: 'Low drive-power integrated acoustooptic filter on X-cut Y-propagating $LiNbO_3$', *IEEE Photonics Technol. Lett.*, 1991, **3**, pp. 923–925

4 DIEULESAINT, E., and ROYER, D.: 'Ondes élastiques dans les solides. Masson et Cie, Éditeurs, 1974

5 BAHR, A.J., and LEE, R.E.: 'Equivalent-circuit model for interdigital transducers with varying electrode widths', *Electron. Lett.*, 1973, **9**, pp. 281–282

6 SLOBODNICK, CONWAY, and DELMONICO (Eds.): 'Microwave acoustics handbook, Vol. B1A, surface wave velocities' (Air Force Cambridge Research Labs, USA, 1973)

7 SMITH, W.R., GERARD, H.M., COLLINS, J.H., REEDER, T.M., and SHAW, H.J.: 'Analysis of interdigital surface wave transducers by use of an equivalent circuit model', *IEEE Trans.*, 1969, **MTT-17**, pp. 856–864

8 GOTO, N., and MIYAZAKI, Y.: 'Integrated optical multi-/demultiplexer using acoustooptic effect for multiwavelength optical communications', *IEEE J. Sel. Areas Commun.*, 1990, **SAC-8**, pp. 1160–1168

9 JOURDAN, A., SOULAGE, G., DA LOURA, G., CLESCA, B., DOUSSIERE, P., DUCHET, C., LECLERT, D., VINCHANT, J.F., and SOTOM, M.: 'Experimental assessment of a 4 × 4 four wavelength all-optical cross-connect at a 10 Gbit/s line rate'. OFC'95, pp. 277–278

Low drive power, sidelobe free acousto-optic tunable filters/switches

C.S. Qin, G.C. Huang, K.T. Chan and K.W. Cheung

Indexing terms: Acousto-optical filters, Integrated optics

A new family of acousto-optic tunable filters (AOTFs) based on collinear beam interaction on TeO_2 are demonstrated. The sidelobes are suppressed by over 33dB and the filters require very low RF drive power (20mW) to operate.

Introduction: Wavelength tunable filters based on acousto-optic interaction have attracted much attention in recent years [1, 2] because of their potential applications as wavelength routing switches and taps in WDM networks [3]. Furthermore, wavelength tunable filters can also be used inside a laser cavity to create a fast, broadly wavelength-tunable laser [4].

In this Letter, a new family of acousto-optic tunable filters with nearly ideal filter characteristics are demonstrated: low drive power (~few mW at 98% conversion efficiency), narrow filter bandwidth (~few Å FWHM), high conversion efficiency (≥ 98% achieved), and most importantly, extremely high sidelobe suppression ratio (SLSR) (≥ 33dB). The SLSR is at least 22dB better than conventional integrated AOTFs [2] and 15dB better than the latest two-stage design [5] or the focused SAW design [6], and is a very important factor in many applications such as suppressing crosstalk in WDM networks.

The design is based on collinear beam interaction on acoustically anisotropic material [7, 8]. Furthermore, our new design can withstand small angular deviations of the acoustic vector, making the present design much easier to realise and manufacture.

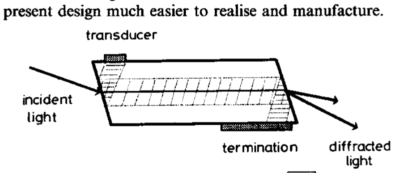

Fig. 1 *Schematic diagram of collinear beam (CB) AOTF*

Filter design: A schematic dagram of the collinear beam (CB) AOTF is shown in Fig. 1. The acousto-optic medium is TeO_2. An $LiNbO_3$ X-cut transducer is bonded on one side of the crystal to excite an acoustic shear wave in the crystal. This acoustic shear wave is reflected from the filter end plane and then propagates with k_a equal to 10.3° from the [110] axis.

Since the acoustic energy (V_g) actually propagates at 65° from the [110] axis due to acoustic wave walkoff, the acoustic energy coincides with the incoming optical beam (k_i). The wave vector diagram is shown in Fig. 2. Thus, the interaction length can be much longer than that of traditional non-collinear filters with the same optical aperture. This significantly reduces the acoustic drive power requirement. In fact, the estimated drive power required for this type of CB-AOTF [8] is comparable to the best integrated AOTFs using acoustic waveguides [5, 6].

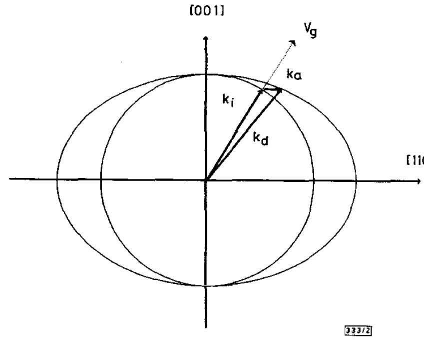

Fig. 2 *Wave vector diagram*

It was also discovered that the previous design of CB-AOTF [8] was very susceptible to small angular deviations of the acoustic vector, which could easily cause a severe degradation in performance. For example, a small angular deviation of the design (say 0.5°) can result in an order of magnitude increase in the drive power required. This has been avoided in our new design.

Filter characteristics: Several filters have been made to verify the validity of the design. Here we present the measured characteristics of one of these filters. The present device is designed to operate around 0.6 – 0.9μm and the characterisation is performed at 0.633μm. The proposed design can be tailored to operate anywhere within the transparency range of TeO_2 simply by redesigning the transducer. The filter characteristic is shown in Fig. 3.

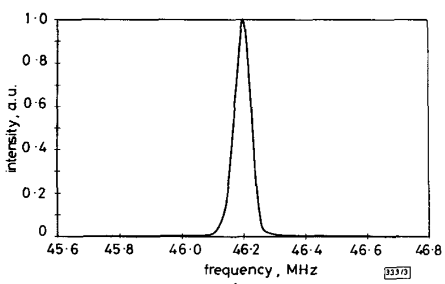

Fig. 3 *Filter characteristics at 0.633Å*

Sidelobes have been suppressed by over 33dB

The RF drive frequency is ~46MHz, and the required RF drive power to achieve 98% conversion efficiency is only 20mW. This low drive power is obtained even without a proper impedance matching of the transducer. Since the transducer loss is measured to be ~16dB at this frequency, we expect that the drive power can be further lowered by an order of magnitude. The 3dB (FWHM) filter bandwidth is ~8Å and the 20dB filter full-width is ~33Å. The transducer aperture is 2 × 3mm², and the total interaction length is 25mm. The SLSR has been measured to be better than 33dB, and is only limited by the sensitivity of our measuring equipment.

In conclusion, we have demonstrated a new family of AOTFs which have excellent characteristics and extremely high sidelobe suppression ratio. The filters should be useful in many applications including fast tunable lasers and WDM networks.

15 May 1995
Electronics Letters Online No: 19950829

C.S. Qin and K.T. Chan (*Department of Electronic Engineering, The Chinese University of Hong Kong, Shatin, Hong Kong*)

G.C. Huang (*Shanghai Institute of Ceramics, Academia Sinica, Shanghai, People's Republic of China*)

K.W. Cheung (*Department of Information Engineering, The Chinese University of Hong Kong, Shatin, Hong Kong*)

References

1 CHEUNG, K.W., CHOY, M.M., and KOBRINSKI, H.: 'Electronic wavelength tuning using acousto-optic tunable filter with broad continuous tuning range and narrow channel spacing', *IEEE Photonics Technol. Lett.*, 1989, **1**, pp. 38–40
2 SMITH, D.A., BARAN, J.E., JOHNSON, J.J., and CHEUNG, K.W.: 'Integrated-optic acoustically-tunable filters for WDM networks', *IEEE J. Sel. Areas Commun.*, 1990, **SAC-8**, pp. 1151–1159
3 CHEUNG, K.W.: 'Acousto-optic tunable filters in dense WDM networks: System issues and network applications', *IEEE J. Sel. Areas Commun.*, 1990, **SAC-8**, pp. 1015–1025
4 COQUIN, G., and CHEUNG, K.W.: 'Electronically-tunable external-cavity semiconductor laser', *Electron. Lett.*, 1988, **24**, pp. 599–600
5 TIAN, F.: 'Polarization-independent integrated optical, acoustically tunable double-stage wavelength filter in $LiNbO_3$', *J. Lightwave Technol.*, 1994, **LT-12**, pp. 1192–1197
6 KAR-ROY, A., and TSAI, C.S.: 'Low-sidelobe weighted-coupled integrated acoustooptic tunable filter using focused surface acoustic waves', *IEEE Photonics Technol. Lett.*, 1992, **4**, pp. 1132–1135
7 KUSTERS, J.A., WILSON, D.A., and HAMMOND, D.L.: 'Optimum crystal orientation for acousticallly tuned optical filters', *J. Opt. Soc. Am*, 1974, **64**, pp. 434–440
8 CHANG, I.C.: 'Collinear beam acousto-optic tunable filters', *Electron. Lett.*, 1992, **28**, pp. 1255–1256

Low loss channel waveguides fabricated in fused silica by germanium ion implantation

P.W. Leech, P.C. Kemeny and M.C. Ridgway

Indexing terms: Optical waveguides, Silicon dioxide, Ion implantation

The authors report the first low loss channel waveguides (0.10–0.15 dB/cm) formed in fused silica by the implantation of MeV Ge ions. The loss coefficient α was measured as a function of ion dose (8×10^{13} – 8×10^{16} ion/cm²) and annealing temperature (250 to 600°C) at 1300nm. The as-implanted waveguides exhibited a minimum value of α = 0.9dB/cm at an intermediate range of dose with a reduction to 0.10–0.15dB/cm after annealing at 500°C.

The implantation of selected ions (He^+, N^+ and Si^{2+}) into silica glass has been shown to produce a buried layer of increased refractive index as summarised in [1, 2]. Although the implanted layer has been used to define the core region of planar waveguides, there have been few reported measurements of optical loss. Recently, the implantation of MeV Ge ions into silica glass at 300K has produced both an increase in refractive index and an enhancement in optical absorption at 244 and 212nm [3 – 5]. The level of ion-induced optical absorption was reduced by irradiation of the samples with 249nm laser light, thereby enabling the direct writing of gratings in the implanted silica. MeV implantation of fused silica with Ge ions has also recently been used to form slab [5] and channel [6] waveguides. As a result, the potential exists for the fabrication of planar waveguides with incorporated in-core devices. We report the optimisation of the low loss characteristics in Ge implanted waveguides as a function of ion dose and annealing temperature.

The waveguides were formed on substrates of Suprasil II fused silica (10 × 1 × 50mm³). The fabrication process comprised the electrodeposition of a layer of Au (4 μm thick) and the definition of a series of channels [6] (6μm in width and 4cm in length) with smooth sidewalls. This thickness of the masking layer of Au (4μm) was necessary to prevent the penetration of 99.99% of the implanted 5MeV Ge ions. The implantations were performed with all ion beam of intensity 150nA which was rastered across the surface of the sample. The target doses ranged from 10^{14} to 10^{17} ion/cm². A substrate temperature of –196°C was used to reduce the extent of dynamic annealing and hence maximise the increase in refractive index. After implantation, the masking layer of Au was stripped from the surface by a cyanide etch and the ends of the samples were polished.